Influence of spot size on extreme ultraviolet efficiency of laser-produced Sn plasmas

S. S. Harilal,[1,a)] R. W. Coons,[1] P. Hough,[2] and A. Hassanein[1]
[1]*School of Nuclear Engineering and Center for Materials Under Extreme Environment, Purdue University, 400 Central Dr., West Lafayette, Indiana 47907, USA*
[2]*School of Physical Sciences and National Centre for Plasma Science and Technology, Dublin City University, Dublin 9, Ireland*

(Received 15 September 2009; accepted 10 November 2009; published online 30 November 2009)

We have investigated the spot size effects on the extreme ultraviolet conversion efficiency (CE) of CO_2 laser-produced Sn plasmas. The estimated CE of the laser to 13.5 nm radiation, within a 2% bandwidth, using a 10.6 μm CO_2 laser with various pulse widths (25–55 ns) showed a double hump structure during a target-lens scan, where the CE is nearly 25% lower at the best focal position. Density analysis of the CO_2 laser-produced plasma showed steep density gradients at the best focal position, and a reduction in CE at the best focal position, which is explained by the lack of efficient coupling between the laser and the plasma. © *2009 American Institute of Physics*.
[doi:10.1063/1.3270526]

The essential requirement for extreme ultraviolet lithography (EUVL) is to have a reliable, clean, and powerful light source at a wavelength of 13.5 nm. This choice of wavelength is based on the availability of Mo/Si multilayer mirrors that reflect nearly 68% of light centered at 13.5 nm. A laser-produced plasma (LPP) radiation source is one of the most promising options for the EUVL light source.[1] A suitable LPP source will require an efficient conversion of the incident laser pulse energy to EUV radiation in a 2% bandwidth centered on 13.5 nm, as well as a nearly complete control of the debris transport. Developing an EUV source with a high in-band conversion efficiency (CE) is imperative, as this reduces the production and ownership costs of EUVL light source systems. LPP from lithium, xenon, and tin are good emitters in the in-band region near 13.5 nm. Tin plasmas[2,3] are more promising in this context, as they provide a higher CE than lithium[4] or xenon.[5] The reported CE[2,3] from a planar Sn target using a 1064 nm Nd:yttrium aluminum garnet (YAG) laser excitation is around 2% in a solid angle of 2π steradians. However, 10.6 μm CO_2 laser excitation can produce higher CEs (2.5%) for a Sn plasma compared to a YAG laser plasma due to its lower opacity.[6]

The CE of laser-produced Sn plasmas depends on several parameters. Previous reports showed that the CE varies with various laser and target parameters, including laser wavelength,[6] pulse width,[7] intensity,[2] target geometry,[8] target mass density,[2] etc. The properties of LPP also depend on the spot size, as well the focal position with respect to the target-lens distance. Earlier studies showed that the plasma expands spherically with smaller spot sizes, and the expansion changes and becomes more cylindrical with a larger spot size.[9] Kasperczuk *et al.*[10] demonstrated that the focal position can substantially influence the conditions of plasma jet formation due to changes in the laser intensity distribution interacting with a preformed plasma. In this letter, we report the effect of the target-lens position and hence, the spot size, on the CE of CO_2 LPPs. Our results show that the target-lens position is found to be crucial in obtaining the optimal CE.

The schematic of the experimental setup is given in Fig. 1. Pulses from a transversely excited atmospheric CO_2 laser emitting at 10.6 μm is used for producing plasmas on a Sn target. The target is placed at the center of a vacuum chamber pumped using a turbomolecular pump, and a vacuum of $\sim 10^{-6}$ Torr has been achieved. We varied the pulse width of the CO_2 pulse by using a plasma shutter device.[11] The full width at half maximum (FWHM) of the laser pulse is varied from 25–60 ns by varying the separation between the focusing lens and the pinhole in the plasma shutter. The CO_2 laser pulses are focused onto the target using a f/10 or f/5 meniscus ZnSe lens. All experiments were performed in a single-shot mode. We used an absolutely calibrated instrument (Power Tool) for measuring the conversion of the laser energy to 13.5 nm with a 2% bandwidth, commonly known as in-band energy. The power tool consists of two Zr filters, one Mo–Si multilayer mirror, and an EUV photodiode (IRD

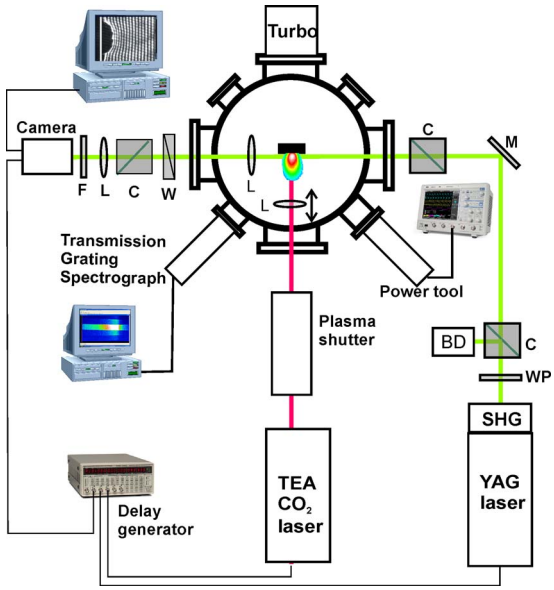

FIG. 1. (Color online) Schematic of the experimental setup. (WP–wave plate; C–cube polarizer; M–mirror; W–Wollaston prism; L–lens; F–filter; BD–beam dump).

a)Electronic mail: sharilal@purdue.edu.

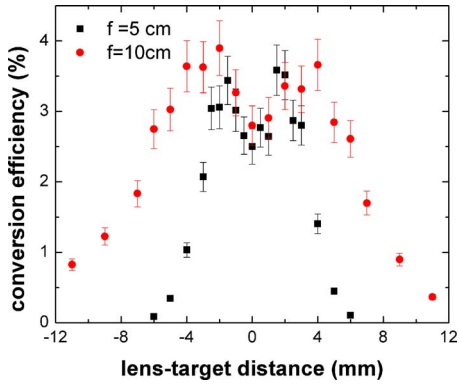

FIG. 2. (Color online) The in-band CE as a function of the lens-target distance for f/10 and f/5 lenses is given. A 25 ns CO_2 laser pulse is used.

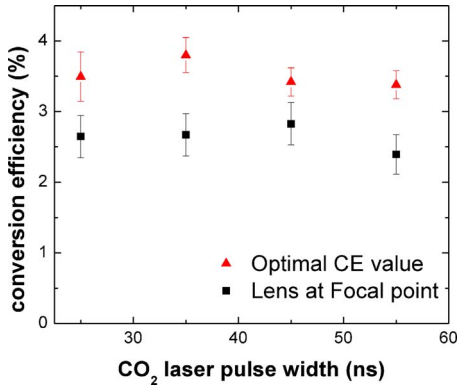

FIG. 3. (Color online) The pulse width effect on the in-band CE of CO2 laser-produced Sn plasma by keeping the lens at the best focal position and the optimal CE value lens position. The power density used at the best focal position was 6 GW/cm^2.

AXUV100). For estimating the CE, we assumed a hemispherical symmetry of the plasma geometry, and that the output from the power tool is integrated over a 2π steradian solid angle. An EUV transmission grating spectrograph with a 10 000 lines/mm grating coupled to a back-illuminated Princeton charge coupled device (Princeton Instruments PIXIS) is used for recording the spectral features of the Sn plasma. Both the spectrograph and energy monitors are attached to the chamber at a 45° angle with respect to the laser beam. A polarization-based Nomarski interferometer is used for recording the density profiles of the plasmas. The probe laser is operated at 532 nm with a 5 ns FWHM. A $\lambda/2$ wave plate and a cube polarizer are used for adjusting the polarization and energy of the probe beam. The probe beam passes through the plasma parallel to the target surface, and the target is imaged onto the detector using a f/10 lens. The Wollaston prism is inserted in front of the detector.

Typically, plasmas emit very strongly in the EUV region when the temperature of the plasma is in the 20–40 eV range. The radiation emitted by plasma can be controlled by fine-tuning the temperature, which is inherently dependent on laser and target properties. The CE of the plasma is strongly dependent on the laser power density. For example, Fig. 2 shows the estimated CE values at various lens positions with respect to the target for a 10.6 μm CO_2 laser with two lenses of focal lengths 5 and 10 cm. The laser energy and pulse width used for these measurements are 65 mJ and 25 ns, respectively. It is interesting to notice that the CE values showed a dip at the best focal position. Hence, the best CE values are obtained at either side of the best focal position. This indicates the most suitable CO_2 laser intensity for the optimum production of EUV radiation is slightly away from the best focal position, where the CE is nearly 25% higher than at the smallest spot size.

Our studies showed that the target-lens scan effect on CE is not dependent on the pulse width of the laser. A similar dip at the best focal position has been noticed with different pulse widths of the CO_2 laser. A plasma shutter device[11] was used for varying the pulse width from 25–55 ns. The pulse width dependence of CE values obtained with the lens at the best focal position and at the best conditions for EUV production is given in Fig. 3, and this indicates that the CE values are nearly 25% higher, regardless of pulse width of the laser if we select the optimal target-lens distance. The laser irradiance at the best focal position was 6 GW/cm^2 for all pulse widths.

We noticed the CE values are nearly 25% lower at the best focal spot. This shows that the smallest spot size is not the optimal condition for obtaining the highest CE. This could be due to several factors affecting the radiation transport, including plasma overheating, energy losses due to plasma lateral expansion, opacity effects, differences in laser-plasma coupling cone angle, etc. In order to check the effect of overheating of the plasma, we recorded the unresolved transition array (UTA) (Ref. 12) at the best focal and at optimal CE lens positions, which are given in Fig. 4. The recorded time-integrated spectra showed hardly any difference. We also examined the effect of CE target-lens scan on various laser energies by attenuating the laser beam. However, the target-lens scan CE trend continued even at lower laser energies, and this indicates the reduction in the CE at the best focal point is not due to overheating.

The nature and characteristics of the LPP strongly depend on the laser irradiance. The estimated spot sizes at the best focal position and optimal CE positions for f=10 cm lens are ~225 and ~325 μm, respectively. Considering these, the laser irradiance at the optimal CE lens position is lowered by a factor of 2 compared with the best focal position. The recorded density contours of the plasma plume are given in Fig. 5 for the best focal point and the optimal CE position. Both of the interferograms were recorded 5 ns after the peak of the CO_2 laser pulse, with an integration time equal to the probe laser pulse width (5 ns FWHM). The

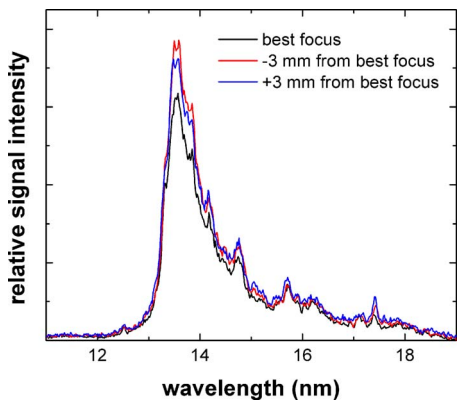

FIG. 4. (Color online) The Sn UTA spectra recorded with different lens positions with respect to the target surface is given. The spectra are time-integrated and a f/10 meniscus lens is used for focusing the CO_2 laser.

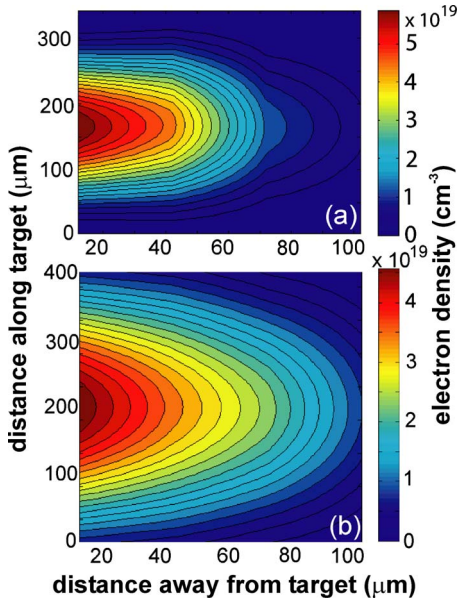

FIG. 5. (Color online) The density profiles recorded 5 ns after the peak of the laser pulse using a Nomarksi interferometer. The density profile is obtained with (a) the best lens focal position and (b) the best CE lens position. A f/10 meniscus lens is used for focusing CO_2 laser.

estimated peak electron densities are 5.8×10^{19} and $4.6\times10^{19}/\mathrm{cm}^3$ for 225 and 325 μm spot sizes, and its values drop rapidly away from the target. Figure 5 also shows that the density gradient is steeper with plasmas produced by a smaller spot size.

It is well known that for nanosecond laser pulses, the leading edge of the laser pulses are used for creating a plasma on the target surface, and the remaining part of the laser pulse energy will be utilized for heating the plasma rather than interacting with the target. It should be noted from Fig. 5 that recorded densities near the target surface are greater than the critical density of the excitation laser beam $(9\times10^{18}/\mathrm{cm}^3)$, and much lower than the probe laser critical density $(3.5\times10^{21}/\mathrm{cm}^3)$. Hence, during the laser pulse, due to the plasma critical density, the absorption front moves away from the target surface, otherwise the plasma will reflect laser photons. Also with a larger spot size, it can be seen that the density profile of the plasma is shifted farther away from the target surface as compared with the density profile obtained with best focal position. This ascertains that most of the heating laser pulse is deposited efficiently at the optimal CE position instead of the steep density profile observed with the best focal position. When the smallest spot size is used, due to the smaller cone angle of the laser beam, the plasma absorption will be localized near the vicinity of the central axis. When the spot size is slightly away from the best focal conditions, the laser cone angle will be larger, and hence, the remaining part of the laser will be efficiently distributed among the entire plasma front. This provides a better laser-plasma coupling, leading to better conditions for EUV production.

In summary, we have investigated the effect of the spot size on the CE of CO_2 laser-produced Sn plasmas. The estimated CE is found to be lower at the best focal position, which showed a double hump profile during the lens scan. The pulse width of the CO_2 laser has a minimal effect on CE when it is varied from 25–60 ns, while a 25% enhancement in the CE is obtained by selecting the best target-lens position. A density analysis of the plasma formed at various lens positions showed a steep density gradient for plasmas formed at the best focal position compared to the density contours recorded at the optimal CE lens position. Hence, a better laser-plasma coupling is expected with a larger scale length of the plasma, which is the case of the optimal CE lens position.

[1] V. Bakshi, *EUV Sources for Lithography* (SPIE, New York, 2006).
[2] S. S. Harilal, M. S. Tillack, B. O'Shay, Y. Tao, and A. Nikroo, Opt. Lett. **31**, 1549 (2006).
[3] Y. Tao, M. S. Tillack, S. S. Harilal, K. L. Sequoia, and F. Najmabadi, J. Appl. Phys. **101**, 023305 (2007).
[4] A. Nagano, T. Inoue, P. E. Nica, S. Amano, S. Miyamoto, and T. Mochizuki, Appl. Phys. Lett. **90**, 151502 (2007).
[5] Y. Ueno, T. Ariga, G. Soumagne, T. Higashiguchi, S. Kubodera, I. Pogorelsky, I. Pavlishin, D. Stolyarov, M. Babzien, K. Kusche, and V. Yakimenko, Appl. Phys. Lett. **90**, 191503 (2007).
[6] J. White, P. Dunne, P. Hayden, F. O'Reilly, and G. O'Sullivan, Appl. Phys. Lett. **90**, 181502 (2007).
[7] T. Ando, S. Fujioka, H. Nishimura, N. Ueda, Y. Yasuda, K. Nagai, T. Norimatsu, M. Murakami, K. Nishihara, N. Miyanaga, Y. Izawa, K. Mima, and A. Sunahara, Appl. Phys. Lett. **89**, 151501 (2006).
[8] Y. Ueno, G. Soumagne, A. Sumitani, A. Endo, and T. Higashiguchi, Appl. Phys. Lett. **91**, 231501 (2007).
[9] S. S. Harilal, J. Appl. Phys. **102**, 123306 (2007).
[10] A. Kasperczuk, T. Pisarczyk, M. Kalal, J. Ullschmied, E. Krousky, K. Masek, M. Pfeifer, K. Rohlena, J. Skala, and P. Pisarczyk, Appl. Phys. Lett. **94**, 081501 (2009).
[11] N. Hurst and S. S. Harilal, Rev. Sci. Instrum. **80**, 035101 (2009).
[12] J. White, A. Cummings, P. Dunne, P. Hayden, and G. O'Sullivan, J. Appl. Phys. **101**, 043301 (2007).